Available online at www.sciencedirect.com
SCIENCE DIRECT
Earth and Planetary Science Letters 243 (2006) 282–292
EPSL
www.elsevier.com/locate/epsl

Cooling rate correction of paleointensity determination for volcanic glasses by relaxation geospeedometry

R. Leonhardt *, J. Matzka, A.R.L. Nichols [1], D.B. Dingwell

Department for Earth and Environmental Sciences, Ludwig-Maximilians-University, Munich, Germany

Received 2 August 2005; received in revised form 8 December 2005; accepted 30 December 2005
Available online 14 February 2006
Editor: R.D. van der Hilst

Abstract

The influence of the cooling rate on paleointensity estimates was investigated for samples from a vertical profile across a 600 A.D. obsidian lava flow ramp from Lipari, Italy. The natural cooling rates at the glass transition, which were previously determined for the seven investigated samples by relaxation geospeedometry, vary by a factor of more than 4. Rock magnetic investigations indicate a magnetic microlite fraction in the single-domain grain size range and strong magnetic anisotropy. The thermoremanence anisotropy tensor was determined for each specimen to correct the paleointensity results for this anisotropy. The cooling rate dependency of the thermoremanence was determined experimentally. Extrapolation to natural cooling rates indicate an overestimate of the paleointensity by 13% to 20% during experiments with typical laboratory cooling rates. Correcting for the different cooling rates and the cooling rate dependencies within the vertical profile, significantly reduces the standard deviation of the average flow paleointensity. The average paleointensity for the 543±19 A.D. flow ramp results in 52.4±1.1 μT, corresponding to a virtual axial dipole moment of 9.2±0.2 Am^2. Uncertainties, introduced by anisotropy correction and cooling rate extrapolation, are considered by error propagation.

Keywords: paleointensity; paleomagnetism; geomagnetism; thellier method; volcanic glass; cooling rate; relaxation geospeedometry; obsidian

1. Introduction

It is well known that determinations of paleointensity provide important constraints on the evolution of the Earth's magnetic field on geological and historical timescales [e.g. 1–4]. In general, paleointensity values are much more difficult to obtain than the paleomagnetic directional information of that field. Several mechanisms can cause failure or bias in the determinations of absolute paleointensity. Among these are magnetomineralogical changes during geological time and laboratory treatment [5], magnetic anisotropy of the remanence [6], magnetic domain state bias affecting the different remanence acquisition processes in nature and in the laboratory [7], and different heating/cooling histories [8].

In order to overcome those inherent problems of paleointensity determination, investigations have been carried out to find an ideal paleointensity recorder. It has been suggested that volcanic glass is such an ideal material for intensity determination [e.g. 9,10]. In

* Corresponding author.
E-mail address: leon@geophysik.uni-muenchen.de (R. Leonhardt).
[1] Present address: Institute for Research on Earth Evolution, JAMSTEC, Kanagawa, Japan.

0012-821X/$ - see front matter © 2006 Elsevier B.V. All rights reserved.
doi:10.1016/j.epsl.2005.12.038

particular, Holocene submarine basaltic glass samples show almost ideal properties regarding geological and laboratory alterations as well as domain state [9]. Furthermore, they experience cooling histories comparable to those in the laboratory. Magnetic remanence carriers of volcanic glass samples of various ages are found to be predominantly low-Ti titanomagnetites in the single-domain (SD) size range [9,11–13]. Therefore, a domain state bias to the most commonly used Thellier-type paleointensity determination methods can be excluded. Furthermore, such volcanic glasses appear to be almost pristine, showing little evidence of geological and laboratory alterations.

This finding, however, was questioned by Smirnov and Tarduno [13]. Particularly for Cretaceous submarine basaltic glass, these authors showed that significant laboratory alteration biases the paleointensity determination. The resultant bias towards lower field values might also explain the apparent difference between paleointensity records from glasses and other volcanic rocks older than 0.5 Ma [12,14,15]. It was suggested that such alteration is related to the glass transition temperature interval [13], which is the kinetic boundary across which the glass properties change from that of a solid (brittle deformation) to that of a (super-cooled) liquid (viscous deformation). If this transition occurs below the blocking temperature of the remanence, laboratory heating steps can lead to an alteration of magnetic minerals. This would not necessarily be seen in the alteration checks typically used during Thellier-type intensity experiments [13]. It is important to know, therefore, the temperature interval across which the glass transition occurs when selecting a sample for intensity experiments.

If the natural cooling rate of the volcanic glass is different from the laboratory cooling rates this will significantly affect the reliability of paleointensity values. It has been shown that the extent to which ferrimagnetic particles acquire a natural remanent magnetization (NRM) in the presence of an ambient field is dependent on the cooling rate in the blocking temperature interval [e.g. 8,16]. For SD particles, faster cooling leads to weaker TRMs. Therefore, very slow cooling rates relative to the laboratory timescales might give paleointensity overestimates of more than 20% [16]. For volcanic glass, significant differences in cooling rate are to be expected depending on the composition, volcanic facies and quenching environment. Known values for the natural cooling rate and the cooling rate dependency of TRM would enable an estimation of the possible bias and allow the paleointensity values to be corrected.

Natural cooling rates of vitreous materials can be determined across the glass transition using relaxation geospeedometry. This involves measuring the specific heat capacity (c_p) of the glass during several heating/cooling cycles using a differential scanning calorimeter (DSC). The variation of c_p with temperature depends on the cooling and subsequent heating rates. A single glass transition temperature (T_g) can be defined for each cooling and heating rate, for example as the temperature at which the peak in c_p occurs across the glass transition. By modeling the c_p curves where both cooling and heating rate are known following the Tool–Narayanaswamy approach [17,18], using the procedure outlined by [19], a set of sample specific parameters are obtained. These are then used to model the c_p curve measured on initial heating of the sample, enabling the natural cooling rate across the glass transition to be defined.

Bowles et al. [20] have already compared laboratory cooling rates, used in paleointensity measurements, with natural cooling rates, determined by relaxation geospeedometry, in Holocene submarine basaltic samples. Since the differences in the cooling rates were negligible they found no bias in the paleointensity determinations.

Here we present rock magnetic and paleointensity results from slowly cooled, subaerial volcanic glass samples, for which cooling rates have already been determined by relaxation geospeedometry [21]. These obsidian samples consist of a glassy matrix containing microlites. The domain state, thermal stability, anisotropy, and magnetic cooling rate dependency of the ferrimagnetic microlites is determined. Using the natural cooling rates obtained by relaxation geospeedometry, the effect of cooling rate bias on paleointensity determination is investigated and corrected for.

2. Sample description

Samples used in this study come from the Rocche Rosse obsidian flow. This rhyolite flow was extruded in the sixth century A.D., historic sources suggest between 524 A.D. and 562 A.D., on the northern coast of Lipari, Aeolian Islands, Italy [22]. In order to investigate the cooling history of flow ramps, unoriented samples were taken using a portable, gasoline driven drill in a vertical profile 190 cm high and 4 m wide. These samples were subjected to mineralogical and calorimetric investigations [profile P3RR, 21] to determine both T_g and the natural cooling rates across the glass transition. T_g vary between 675 and 705 °C. Specimens for the magnetic study were taken from the same samples that were used by Gottsmann and Dingwell [21], which

comprise seven different vertical positions within a flow ramp. Drill cores 5 mm in diameter were taken from each cylinder and cut into two 4–5 mm long pieces. One piece was subjected to a set of rock magnetic measurements. The other was used for paleointensity determination and then the anisotropy of the thermoremanent magnetization (ATRM) and the magnetic cooling rate dependency were analyzed.

2.1. Magnetic mineralogy and domain state

Rock magnetic measurements aimed to identify the magnetic mineralogy and domain state. Isothermal remanent magnetization (IRM) acquisition, hysteresis loops, isothermal backfield curves at room temperature, and thermomagnetic curves (giving values for the magnetic field, B, of 500 mT; and the maximum temperature, T_{max}, of 600 °C) were measured in that order. After the thermomagnetic measurement, the hysteresis and backfield measurements were repeated in order to test the thermal stability of the samples. All measurements were conducted using a Variable Field Translation Balance (VFTB).

Thermomagnetic curves yield Curie temperatures (T_C) of ≈550 °C for all specimens. Heating and cooling curves are reversible, indicating that alteration does not occur. The pristine character of the specimens is further supported by hysteresis and backfield measurements, which are almost identical before and after the heating experiment (Fig. 1a–c).

According to Day et al. [23] and Dunlop [24], the domain state related ratios of coercivity of remanence versus coercive force (B_{cr}/B_c) (Fig. 1b) and saturation remanence versus saturation magnetization (M_{rs}/M_s) (Fig. 1c) indicate average grain sizes in pseudo-single- (PSD) to multi-domain (MD) ranges. However, with the exception of the uppermost specimen, uniformly high B_{cr} are observed (Fig. 1a), pointing to a SD grain size range. In order to clarify the magnetic domain state of the remanence carrying particles, and thus the suitability of the samples for paleointensity determination, magnetization tails of partial thermoremanent magnetizations (pTRM) were investigated. The magnitude of demagnetization tails is characteristic for the domain state [25–27]. Tail measurements of pTRM were conducted in the course of the Thellier-type experiments, using the repeated demagnetization steps after pTRM acquisition [28]. pTRM acquisition in Theller experiments is different to the traditional pTRM definition, since the maximum temperature at which a laboratory field is applied is not reached from T_C. Therefore, hereafter pTRM∗ is used as an abbreviation. The maximum intensity differences between primary and repeated demagnetization (δ(TR)) are shown as grey bars in Fig. 1d. From this intensity difference and the angular difference between the applied field and the natural magnetization of the specimen, the extent of the 'true' tail of pTRM∗ ($\delta(t*)$) is calculated [7] and shown as black bars in Fig. 1d. [7]. Leonhardt et al. related the extent of $\delta(t*)$ to the thermomagnetic criterion [29] and, thus, defined the domain size limits indicated in Fig. 1d. In agreement with the high B_{cr}, the tails provide evidence for the dominantly SD character of the remanence carrying particles.

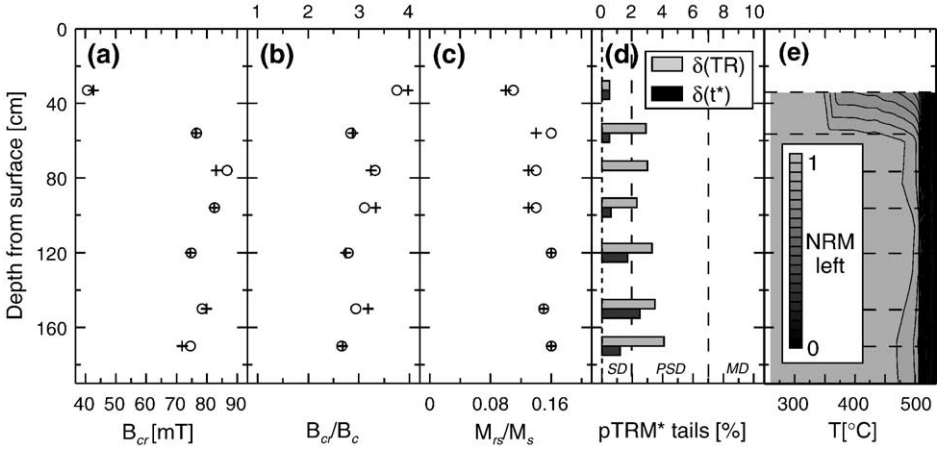

Fig. 1. Rock magnetic parameters across the obsidian flow profile. Plus symbols in (a), (b) and (c) denote hysteresis parameters measured prior to heating the sample to 600 °C; circles show post-heating results. Relative intensity differences in pTRM∗ tail checks, measured at 530 °C, and corresponding $\delta(t*)$'s are shown in (d) as grey and black bars, respectively. Domain state estimates for the black bars are related to the thermomagnetic criterion [7]. The unblocking characteristic is shown in (e), indicating sharp unblocking between 500 and 550 °C.

Since the behavior of the magnetic remanence is incompatible with the hysteresis ratios, B_{cr}/B_c and M_{rs}/M_s, which are partly influenced by the induced magnetization, the rock magnetic parameters suggest that two types of magnetic microlites are present in the samples. One type, microlite fraction *A*, is likely to be in the single-domain grain size range (approx. 0.05 to 1 μm for magnetite [30]) and carries the dominant part of the remanent magnetization of the samples. The other type, referred to as microlite fraction *B*, is in the multidomain grain size range and affects the induced magnetization, but has a minor effect on the samples remanent magnetization.

The NRM unblocking temperature of around 550 °C (Fig. 1e) indicates that the microlite fraction *A* is an impure magnetite. Assuming that the impurity is Ti, the unblocking temperature corresponds to a titanomagnetite $Fe_{3-x}Ti_xO_4$ with $x=0.05$ [31] in the single-domain grain size range. The magnitude of B_{cr}, which is also a remanence parameter, is too high for equidimensional particles and suggests that the particles are elongated and that the magnetic stability is controlled by shape anisotropy. A third alternative, not discussed in great detail here, would be that the magnitude of B_{cr} is controlled by stress. However, from the well studied properties of the titanomagnetite solid solution series [e.g. 32], it is very likely that this would necessitate internal stress higher than 50 MPa. The narrow unblocking temperature spectrum (Fig. 1e) indicates that microlite fraction *A* is rather homogeneous in terms of composition, grain size, and elongation within each sample, again with the exception of the uppermost sample.

Judging from T_C, the multidomain grains of magnetic microlite fraction *B*, which have a negligible effect on the magnetic remanence, have the same composition as microlite fraction *A* for our samples from the Rocche Rosso flow. Large magnetite and titanomagnetite microlites, on the order of several 10 to 100 μm in size, which would qualify as multidomain particles, have been microscopically identified in volcanic glasses [11,33].

These studies also found smaller microlites, equivalent to our fraction *A*, in their silicic volcanic glass. Geissman et al. [11] studied the Oligocene Mickey Pass ash flow tuff, from the Basin and Range province, western United States, and microscopically identified single crystal, spinel structure Fe-oxides. These were approximately 0.1 to 1 μm in size, with aspect ratios from approximately 1 up to 0.16. Combined with the magnetic properties of their samples (B_{cr}=40 to 60 mT, T_C=550 to 565 °C) these particles were identified as single-domain and pseudo-single-domain magnetite with minor amounts of Ti, Mg, Mn and Cr. There is a clear trend to elongated particles. Schlinger et al. [33], also working on samples from the Basin and Range province, identified uniformly distributed, regular shaped magnetite microlites (with minor amounts of Ti, Cr, Mn). They observed large magnetite needles (around 1 μm and larger) with a preferred orientation in the same plane as the eutaxitic structures. For a sample from the same stratigraphic level in the Tiva Canyon member, Schlinger et al. [34] measured a coercive force of B_{cr}=75.5 mT, which compares well with the B_{cr} of our samples from Rocche Rosse, and identified clusters of SD magnetite needles with a mean aspect ration of 0.07 and length of 0.57 μm.

The work discussed above suggests that the rock magnetic parameters of our samples from the Rocche Rosse flow might be anisotropic [see also 35]. Higher values for B_{cr} might reflect longer, and therefore more elongated needle shaped SD particles.

In summary, the ferrimagnetic microlites bearing the remanence can be referred to as Ti-poor titanomagnetite of homogeneous composition, characterized by dominating SD behavior. Blocking temperatures are well below T_g. The obsidian samples are thermally stable, at least up to 600 °C. Despite an expected strong magnetic shape anisotropy, the samples appear to be ideal recorders of the past geomagnetic field.

2.2. Paleointensity determination

In order to determine the strength of the past geomagnetic field, the samples were subjected to Thellier-type paleointensity experiments. All paleointensity determinations were conducted in a MMTD20 thermal demagnetizer. Laboratory fields of 30 μT were used for all measurements, with a field accuracy of 0.1 μT. Intensity determinations were performed with the modified Thellier-technique MT4 [36], which is a zero-field first method that includes the commonly used pTRM∗ check, the additivity checks [37], and pTRM∗-tail checks [28]. Directional differences between the applied field and the NRM of the pTRM∗-tail check are taken into account [7]. The pTRM∗ checks were conducted "in-field" after the demagnetization step. The laboratory field was applied during heating and cooling. All determinations were analyzed with the ThellierTool4.0 software using the default criteria [36]. Results from two specimens are shown in Fig. 2.

In general, the quality of the individual determinations is very good. All measurements were analyzed between 300 and 570 °C, comprising 11 successive data

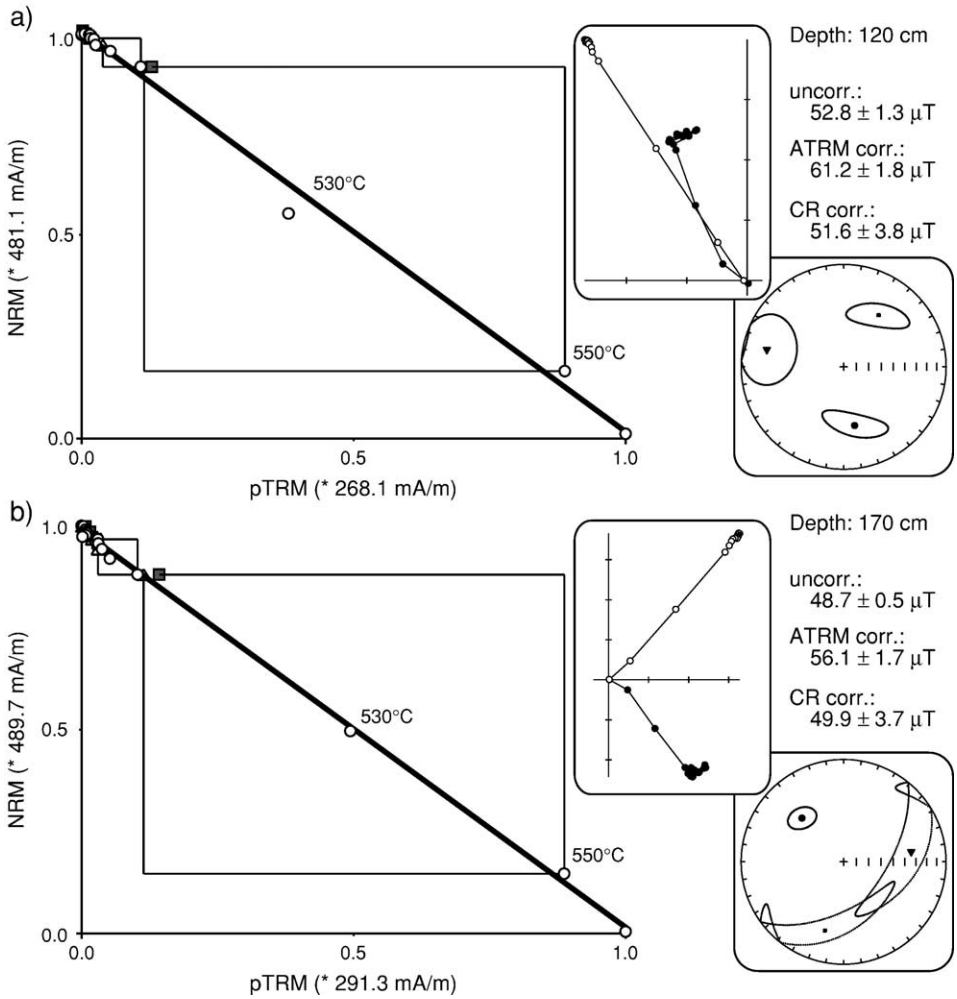

Fig. 2. NRM/pTRM diagrams for two samples from the Rocche Rosse flow. The upper panels to the right show the orthogonal projection of demagnetization steps, where open symbols represent projections on the vertical plane and solid symbols represent the horizontal plane. The lower panels give the principle axes of the ATRM tensor with uncertainty ellipsoids. Both insets use the specimens' core coordinates. Sample (a) is from the central part of the flow and cooled relatively slowly, (b) is the lowermost sample from the profile and cooled more rapidly. Intensity results are given for uncorrected, ATRM corrected and ATRM plus cooling rate (CR) corrected analysis. Note that the uncertainty for each value is calculated by error propagation.

points and a NRM fraction $f>96\%$. Only sample P3RR-1 (33 cm) has a slightly lower f of 78%, which is related to a weak overprint below 250 °C (Fig. 1e). Magneto-mineralogical changes monitored by pTRM∗-checks are virtually absent (DRAT<2.4% for all specimens). Quality factors $q>9$ are primarily affected by the relatively low gap factor $g\approx 64\%$, which in turn are related to the sharp unblocking of the remanence between 520 and 550 °C.

2.3. Magnetic anisotropy

A rock's ability to acquire a magnetization in a magnetic field can depend on the direction of this field. All natural rocks are to some extent magnetically anisotropic, which means that their magnetic properties vary with direction. Since the thermoremanence acquired in a weak field is proportional to the field strength, an anisotropy tensor can be determined for the TRM.

The anisotropy tensor of the thermoremanent magnetization (ATRM) was measured by imparting TRMs using in-field heating/cooling cycles to 570 °C subsequently in +z, +y, +x, −x, −y, and −z direction. Here, it is assumed that the anisotropy ellipsoid of the TRM is characteristic for the analyzed temperature interval during paleointensity analysis. This is justified by the fact that even the ratio $B_{\mathrm{lab}}\cdot \mathrm{NRM}/\mathrm{TRM}$ [38] would

result in similar intensity values to those obtained by the Thellier method. The measurements are analyzed principally following the approach of Veitch et al. [6]. After determination of the ATRM tensor, the direction of the ancient field (H_{anc}) is calculated.

$$H_{anc} = \frac{\mathrm{ATRM}^{-1} \cdot \mathrm{M_{ChRM}}}{|\mathrm{ATRM}^{-1} \cdot \mathrm{M_{ChRM}}|} \quad (1)$$

M_{ChRM} is the characteristic magnetization of the segment analyzed in paleointensity determination. The scaling factor f_{ATRM}, used to adjust the measured paleointensity, is finally obtained by the relationship between ancient magnetization acquisition and laboratory magnetization acquisition in dependency of the ATRM tensor (see also [39]).

$$f_{ATRM} = \frac{|\mathrm{ATRM} \cdot H_{anc}|}{|\mathrm{ATRM} \cdot H_{lab}|} \quad (2)$$

Then the ATRM corrected paleointensity value H_{ATRM} is given by:

$$H_{ATRM} = f_{ATRM} \cdot H \quad (3)$$

In order to estimate the effect of measurement uncertainties, the scaling factor f_{ATRM} was not only determined from the averaged axes components but also from separate positive (+x, +y, +z) and negative (−x, −y, −z) measurements. The uncertainty of f_{ATRM} is then obtained by $\sigma(f_{ATRM}) = |f_{ATRM}^{pos} - f_{ATRM}^{neg}|/2$. In order to test for possible alteration during the subsequent TRM acquisitions, the +z step was repeated after the ATRM determination. A comparison of these two +z acquisitions indicates that little alteration occurred (Fig. 3).

The anisotropy of the investigated glass samples is very strong. Anisotropy factors P are generally above 2 (Fig. 4a). The resultant scaling factors f_{ATRM} range from 0.95 to 1.3 (Table 1). Correcting with f_{ATRM} significantly decreases the variation of paleointensity across the profile (Fig. 4b, Table 1).

2.4. Cooling rate dependency

After application of the ATRM correction, one might expect that the resulting paleointensity variation across the profile might already reflect the differences in natural cooling rates (Fig. 4d). The cooling rate dependency of TRM acquisition, however, is not constant, but related to the domain state and magnetic interactions [40]. Theoretically [16,41] and experimentally [8,40] it was found that an assemblage of identical, non-interacting SD particles acquires a larger TRM during slower cooling. Negative interactions and/or MD kinetics, however, lead to a lower TRM after slower cooling rates [40].

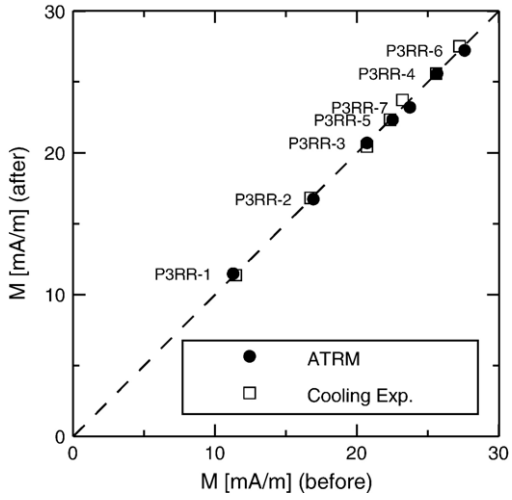

Fig. 3. TRM of individual samples from the profile measured before and after (cooling rate experiment) ATRM determination. The fact that there is very little deviation between the two measurements emphasizes the pristine character of the samples.

Rock magnetic measurements indicate a SD dominance in the samples from Rocche Rosse but small variations of $\delta t*$ across the profile also emphasize that the domain state is not homogeneous. Therefore, following the ATRM determination, all specimens were subjected to magnetic cooling rate dependency investigations. In a first step, the TRM was acquired in a fast heating/cooling cycle ($TRM_{f,l}$) with a cooling rate of ≈240 K/min, which was also used for the paleointensity determinations. In a second step, the in-field heating/cooling cycle was repeated with a 34 times lower cooling rate of 7.1 K/min ($TRM_{s,l}$). Finally, the fast heating cooling cycle was repeated in order to check for any alterations during the experiments (Fig. 3).

Fast cooling was achieved using the MMTD20 furnace with a built in cooling fan, slow cooling was undertaken without fan support. The laboratory cooling rates need to be determined across the same temperature interval as the glass transition, i.e. between 700 and 650 °C for our samples. The cooling rates of our furnace in this temperature range were determined by placing basaltic dummy samples within the sample holder, and monitoring the temperature decrease, indicated by the thermocouple, versus time. The obtained cooling rates are thought to be a good approximation for the TRM experiments on the glasses that were only heated to $T_{max} = 570$ °C.

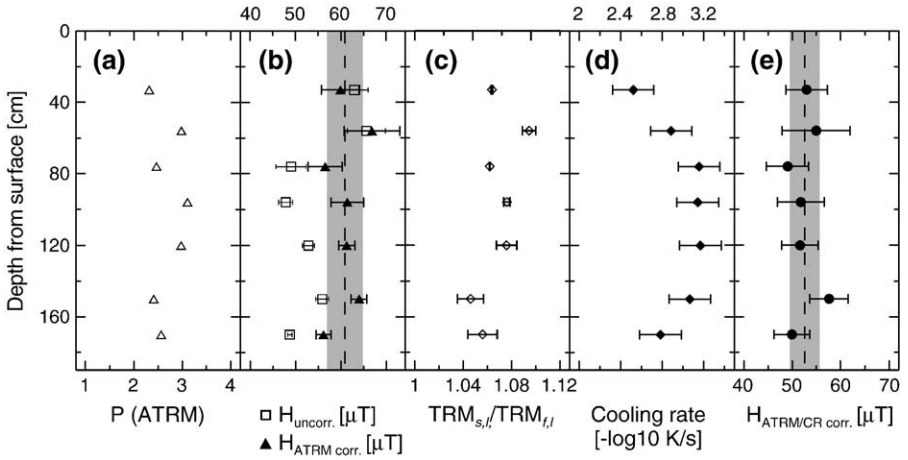

Fig. 4. Intensity determinations and parameters related to ATRM and cooling rate correction across the sampled profile. (a) Shows the magnetic anisotropy factors *P*, which are all above 2, indicating strong magnetic anisotropy. (b) Depicts uncorrected intensity determinations (squares) and ATRM corrected paleointensities (triangles). Also shown is the average ATRM corrected intensity and its corresponding uncertainty. (c) The magnetic cooling rate dependency, expressed by the ratio of TRM acquisition between slow and fast laboratory cooling rates. (d) Natural cooling rates obtained by relaxation geospeedometry. (e) Paleointensity values corrected for both the ATRM and the magnetic cooling rate dependency using the natural cooling rates together with the non-weighted average intensity and its uncertainty.

The TRM intensity is 5% to 10% larger for slow cooling experiments (Fig. 4d), as would be expected for a non-interacting SD assemblage [16,41]. The cooling rate dependency is not uniform across the profile. $TRM_{s,l}/TRM_{f,l}$ decreases with profile depth. This is in agreement with the tail-related domain state analysis, which also yields a slight increase in average domain size with depth (Fig. 1d). Thus, a simple correlation of ATRM corrected paleointensities with natural cooling rate differences in the vertical profile is not seen (Fig. 4b, d). In order to correct the obtained paleointensities for the natural cooling rates, one has to extrapolate the magnetic cooling rate dependency to the natural cooling rates as determined by relaxation geospeedometry. For this purpose, the laboratory measured $TRM_{f,l}$ and $TRM_{s,l}$, both normalized to $TRM_{f,l}$ are plotted versus $\ln(\dot{T}_{f,l}/\dot{T})$ (Fig. 5). A linear relationship between those parameters is to be expected if the remanence is carried by non-interacting SD particles, which are dominantly blocking close to the respective blocking temperature [16]. These conditions are fulfilled for our specimens (Fig. 1d,e). For uncertainty analysis, we estimated the inaccuracy of the laboratory cooling rate determination. A conservative estimate of these errors is 10% for fast cooling and 5% for slow cooling. The relative TRM differences between initial and repeated $TRM_{f,l}$ are assumed to represent the

Table 1
Paleointensity results and correction factors

Depth 1(cm)	Specimen	*T* range (°C)	*f*	g	q	H (μT)	f_{ATRM}	H_{ATRM} (μT)	f_{CR}	$H_{ATRM,CR}$ (μT)
33	p3rr-1	300–570	0.78	0.57	9.1	62.9±3.1	0.951±0.018	59.9±4.2	1.130±0.011	52.9±4.3
56	p3rr-2	300–570	1.00	0.62	9.7	65.6±4.2	1.019±0.030	66.8±6.1	1.216±0.024	54.9±7.0
76	p3rr-3	300–570	0.96	0.61	8.6	49.0±3.3	1.154±0.009	56.5±3.8	1.152±0.010	49.0±4.4
96	p3rr-4	300–570	0.99	0.64	19.8	47.8±1.5	1.285±0.044	61.4±3.6	1.186±0.018	51.7±4.8
120	p3rr-5	300–570	0.98	0.67	26.2	52.8±1.3	1.160±0.009	61.2±1.8	1.187±0.033	51.6±3.8
150	p3rr-6	300–570	1.00	0.67	26.2	55.9±1.4	1.145±0.006	64.0±1.7	1.111±0.034	57.6±3.9
170	p3rr-7	300–570	0.98	0.68	67.6	48.7±0.5	1.152±0.025	56.1±1.7	1.124±0.036	49.9±3.7
Arithmetic average:						54.7±7.2		60.8±3.8		52.5±2.9
Weighted average:										52.4±1.1

T range specifies the temperature range of the straight line segment used for intensity determination. The fraction of the NRM (*f*), the gap factor (*g*) and the quality factor (*q*) were calculated according to Coe et al. [51]. *H*, H_{ATRM} and $H_{ATRM,CR}$ are the paleointensity values with associated uncertainties for the uncorrected, ATRM corrected and ATRM plus cooling rate (CR) corrected determinations, respectively. Uncertainties are determined by error propagation and include the scatter about the straight line segment, the uncertainty of the ATRM scaling factor (f_{ATRM}) and the uncertainty related to the cooling rate correction factor (f_{CR}). Also shown are arithmetic averages of the intensity values and associated uncertainties. Using $1/\sigma$ as a weighting parameter, the weighted average and uncertainty for the $H_{ATRM,CR}$ are given.

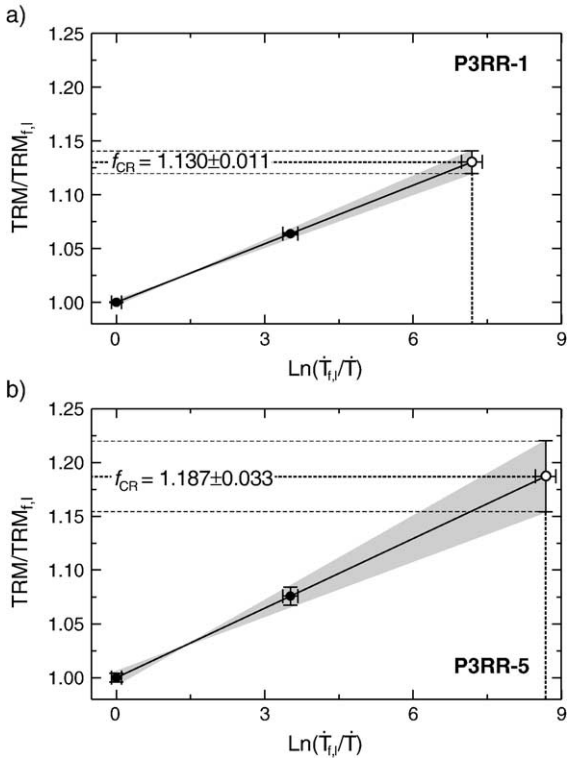

Fig. 5. Cooling rate correction using the laboratory measured cooling rate dependency (solid symbols) and related uncertainties, as well as the linear extrapolation to the natural cooling rate obtained by relaxation geospeedometry (open symbols). (a) Shows a rapidly cooled specimen from the boundary of the flow (33 cm), (b) depicts a slowly cooled sample from the central part (120 cm).

possible inaccuracy of magnetization determination for both $TRM_{f,l}$ and $TRM_{s,l}$. These error estimates allow for a minimum/maximum error propagation towards the natural cooling rates (Fig. 5). The obtained f_{CR} on the $TRM/TRM_{f,l}$ axis is then used to correct the paleointensity values (Table 1).

$$H_{ATRM,CR} = \frac{H_{ATRM}}{f_{CR}} \quad (4)$$

The final paleointensities are significantly lower than the ATRM corrected values. Furthermore, the application of this correction scheme leads to a reduction of the within-profile arithmetic standard deviation of paleointensity (Table 1, Fig. 4e) in comparison to the ATRM corrected values.

3. Discussion and conclusion

Calorimetric measurements of volcanic glass provide two important physical boundary values for the analysis of absolute paleointensity. First, the glass transition temperature (T_g) can be defined, which indicates the transition of viscous (liquid-like) to brittle (solid-like) stress compensation. The glass transition needs to be well above the blocking temperature of the magnetic remanence bearing minerals. If the glass transition occurs at temperatures below the magnetic blocking temperature during primary cooling of the volcanic glass, a reorientation of thermally acquired magnetic moments can occur. Therefore, one cannot unambiguously assume the remanence being exclusively carried by a TRM. This violation of Thellier's first law precludes successful paleointensity determinations. T_g for our investigated samples (675 to 705 °C) are well above the blocking temperatures (~550 °C). Therefore, at least according to this criterion, the samples are suitable for paleointensity determinations.

A number of relaxation geospeedometry measurements on natural volcanic glasses of different composition and volcanic facies revealed T_g ranging from below 450 to 750 °C [42–46]. Furthermore, the structural properties of volcanic glasses may change considerably on geological timescales, since glasses are thermodynamically unstable and tend to devitrify. In particular, hydration can lead to a lowering of T_g. Apparently low T_g<450 °C were found in Cretaceous submarine basaltic glasses [13]. During paleointensity experiments these glasses underwent partial melting and a neocrystallization of ferrimagnetic particles leading to an increase pTRM∗ capacity and thus a bias towards lower paleointensity values. This emphasizes the necessity to know T_g for paleointensity determinations, which can be determined, for example, by calorimetric measurements or from monitoring alterations by hysteresis measurements [13].

The second important piece of information that can be obtained from calorimetric measurements is the natural cooling rate through the glass transition. This is necessary to correct the intensity determination conducted on laboratory timescales. To date cooling rates of natural glasses through this transition have been found to range from 140 to 0.001 K/min. The highest values were measured in rapidly cooled pahoehoe crusts [46]. The lowest values were obtained in spatter-fed lava flows [45] and welded tuffs. Fast cooling during paleointensity determination results in cooling rates comparable to the upper limit of the naturally observed rates, in our experimental setup ≈240 K/min in a temperature range similar to that of the glass transition. Such high natural cooling rates, comparable to the laboratory rates used for paleointensity determination were observed for submarine basaltic glass [20]. The

natural cooling rates for the Rocche Rosse obsidian flow investigated here are considerably smaller, ranging from 0.18 to 0.04 K/min. Such low cooling rates, compared to those of the laboratory, would lead to paleointensity overestimates of 12% to 22% (Table 1) and thus to a significant bias of the paleointensity determination towards higher geomagnetic field values.

Our investigated samples yield 5% to 10% larger TRM acquisition values using a factor of 34 lower laboratory cooling rates. Such values are typically expected for SD behavior [16,41]. This domain state estimate of the remanence contributing magnetic grains is further documented by the small extent of the magnetization tails recorded during the Thellier experiments. Based on these two independent measurements we conclude that the remanence of the obsidian from the Rocche Rosse flow is dominated by SD behavior, similar to that observed in many other studies on volcanic glass [e.g. 9,11,13,34]. Such SD characteristics, however, are not found by bulk rock magnetic measurements. Hysteresis properties are affected by a few large grains, thus resulting in PSD/MD grain size range. These large grains, however, do not significantly affect the remanence acquisition and therefore they do not affect the paleointensity determination either.

ATRM determinations indicated a very strong magnetic anisotropy, which is likely to be related to these elongated magnetic particles. The strong magnetic anisotropy leads to intensity deviations of up to 30%, which is dependent on the angular difference between laboratory and natural field acquisition. For paleointensity determination, such anisotropy can be accounted for in two ways: either the ATRM tensor is determined and the intensity determinations are corrected, as performed here, or field deviations are minimized by conducting the pTRM∗ acquisition steps parallel to the NRM of the sample.

High B_{cr} values are commonly observed in volcanic glass, both in silicic [11,47] and in basaltic glasses [13,48–50]. As outlined already, such high values of B_{cr} are incompatible with equidimensional Ti-poor titanomagnetites. The presence of a magnetic anisotropy affecting the remanence acquisition, both in nature and in the laboratory, can lead to large deviations between individual paleointensity determinations of the same rock, simply because the magnetic fields are differently oriented with respect to the anisotropy tensor. In addition to other mechanisms, like strong local field anomalies, such an anisotropy related intensity bias might at least partly affect large intensity deviations found in recent submarine basaltic glasses [49]. Hence, we suggest that ATRM tensors should be routinely determined in paleomagnetic analysis of volcanic glass.

Both the corrections for anisotropy and the cooling rate difference involve additional measurements and thus also additional sources of uncertainties which finally affect the resultant paleointensity values. In order to account for uncertainties related to the ATRM experiment, the correction factor f_{ATRM} is determined both from only positive and only negative axes measurements. This technique allows deviations in sample orientation and magnetomineralogical changes between those measurements to be estimated. Avoiding a full treatment of tensor uncertainty analysis, this provides a reasonable method to estimate uncertainties related to measurement redundancy. In addition, the extrapolation towards the natural cooling rate is affected by uncertainties. The quality of any extrapolation is heavily dependent on the accuracy of the primary data and validity of the function used for extrapolation. The linear extrapolation in Fig. 5 is justified for the narrow unblocking spectra of our samples [16]. Uncertainties in the laboratory cooling rate and in the TRM acquisition experiment are conservative estimates. An extrapolation of these uncertainties towards the natural cooling rates (Fig. 5) gives a realistic upper limit for the error associated with our cooling rate correction. The accuracy of individual paleointensity determinations is related to the overall uncertainty, σ, which is the sum of the uncertainties caused by deviations from the straight line segment, f_{ATRM} correction and f_{CR} correction. Therefore, $1/\sigma$ is used as a weighting parameter to determine the weighted average paleointensity of the Rocche Rosse flow.

The investigated obsidian flow, historically dated to 543 ± 19 A.D., reveals an intensity of 52.4 ± 1.1 μT, which corresponds to a virtual axial dipole moment (VADM) of $9.2 \pm 0.2 \cdot 10^{22}$ Am^2. This VADM is slightly lower than the dipole moments obtained in archeomagnetic data (western Europe) from 460 A.D. ($9.8 \cdot 10^{22}$ Am^2) and 725 A.D. ($10.1 \cdot 1022$ Am^2) [1]. Our study shows that, along with archeological material, volcanic glasses can be particularly suitable for the reconstruction of historic geomagnetic field variations. At least the silicic glass samples from the Rocche Rosse flow have almost ideal properties regarding paleointensity determination. Whether such ideal properties are generally found in silicic glasses, however, needs to be tested on a larger collection of samples. Despite having not been conducted in our investigation, it is also possible to obtain the direction of that field by taking oriented samples. This is not possible for potsherds, which are the most widely used archeological material for intensity determination.

Deposits of volcanic glasses occur globally and can be very well dated, sometimes even by radiocarbon ages [e.g. 45]. Finally, volcanic rocks recorded the archeomagnetic field at the place of their occurrence. In contrast, some archeological materials might have been transported over long distances from the place where they originally acquired their TRM.

Acknowledgements

We would like to thank the referees for their helpful and constructive comments on the manuscript. Anisotropy analysis was partly conducted with the Pmag1.8.5 analysis software of Lisa Tauxe. Research was funded by the German Science Foundation in the framework of the priority program "Geomagnetic Variations" (So72/67-4 (R.L.)).

References

[1] A. Genevey, Y. Gallet, Intensity of the geomagnetic field in western Europe over the past 2000 years: new data from ancient French pottery, J. Geophys. Res. 107 (2002) EPM1.1–EPM1.17.
[2] V.P. Shcherbakov, G.M. Solodovnikov, N.K. Sycheva, Variations in the geomagnetic dipole during the past 400 million years (Volcanic rocks), Izv. Acad. Sci. USSR Phys. Solid Earth, Engl. Trans. 38 (2002) 113–119.
[3] R. Heller, R.T. Merrill, P.L. McFadden, The two states of paleomagnetic field intensities for the past 320 million years, Phys. Earth Planet. Inter. 135 (2003) 211–223.
[4] J.-P. Valet, Time variations in geomagnetic intensity, Rev. Geophys. 41 (2003), doi:10.1029/2001RG000104.
[5] J.-P. Valet, J. Brassart, I. Le Meur, V. Soler, X. Quidelleur, E. Tric, P.-Y. Gillot, Absolute paleointensity and magnetomineralogical changes, J. Geophys. Res. 101 (1996) 25029–25044.
[6] R.J. Veitch, I.G. Hedley, J.-J. Wagner, An investigation of the intensity of the geomagnetic field during Roman times using magnetically anisotropic bricks and tiles, Arch. Sci. Genéve 37 (1984) 359–373.
[7] R. Leonhardt, D. Krása, R.S. Coe, Multidomain behavior during Thellier paleointensity experiments: a phenomenological model, Phys. Earth Planet. Inter. 147 (2004) 127–140.
[8] J.M.W. Fox, M.J. Aitken, Cooling-rate dependency of thermoremanent magnetisation, Nature 283 (1980) 462–463.
[9] T. Pick, L. Tauxe, Geomagnetic paleointensities: Thellier experiments on submarine basaltic glass from the East Pacific Rise, J. Geophys. Res. 98 (1993) 17949–17964.
[10] P.A. Selkin, L. Tauxe, Long-term variations in paleointensity, Philos. Trans. R. Soc. Lond. 358 (2000) 1065–1088.
[11] J.W. Geissman, N.G. Newberry, D.R. Peacor, Discrete single-domian and pseudo-single-domain titanomagnetite particles in silicic glass of an ash flow tuff, Can. J. Earth Sci. 20 (1983) 334–338.
[12] M.T. Juárez, L. Tauxe, J.S. Gee, T. Pick, The intensity of the Earth's magnetic field over the past 160 million years, Nature 394 (1998) 878–881.
[13] A.V. Smirnov, J.A. Tarduno, Magnetic hysteresis monitoring of Cretaceous submarine basaltic glass during Thellier paleointensity experiments: evidence for alteration and attendant low field bias, Earth Planet. Sci. Lett. 206 (2003) 571–585.
[14] R. Heller, R.T. Merrill, P.L. McFadden, The variation of intensity of the Earth's magnetic field with time, Phys. Earth Planet. Inter. 131 (2002) 237–249.
[15] R. Leonhardt, J. Matzka, E.A. Menor, Absolute paleointensities and paleodirections from Fernando de Noronha, Brazil, Phys. Earth Planet. Inter. 139 (2003) 285–303.
[16] S.L. Halgedahl, R. Day, M. Fuller, The effect of cooling rate on the intensity of weak-field TRM in single-domain magnetite, J. Geophys. Res. 85 (1980) 3690–3698.
[17] O.S. Narayanaswamy, A model of structural relaxation in glass, J. Am. Ceram. Soc. 54 (1971) 491–498.
[18] O.S. Narayanaswamy, Thermorheological simplicity in the glass transition, J. Am. Ceram. Soc. 71 (1988) 900–904.
[19] M.C. Wilding, S.L. Webb, D.B. Dingwell, Evaluation of a relaxation geospeedometer for volcanic glasses, Chem. Geol. 125 (1995) 137–148.
[20] J. Bowles, J.S. Gee, D.V. Kent, E. Bergmanis, J. Sinton, Cooling rate effects on paleointensity estimates in submarine basaltic glass and implications for dating young flows, Geochem. Geophys. Geosyst. 6 (2005) Q07002, doi:10.1029/2004GC000900.
[21] J. Gottsmann, D.B. Dingwell, The cooling of frontal flow ramps: a calorimetric study on the Rocche Rosse rhyolite flow, Lipari, Aeolian Islands, Italy, Terra Nova 13 (2001) 157–164.
[22] H. Pichler, Italienische Vulkangebiete III: Lipari, Vulcano, Stromboli, Tyrrhenisches Meer, in: Sammlung Geologischer Führer, Borntraeger, Berlin, vol. 69, p. 272.
[23] R. Day, M.D. Fuller, V.A. Schmidt, Hysteresis properties of titanomagnetites: grain size and composition dependence, Phys. Earth Planet. Inter. 13 (1977) 260–266.
[24] D. Dunlop, Theory and application of the Day plot (M_{rs}/M_s versus H_{cr}/H_c) 1. Theoretical curves and tests using titanomagnetite data, J. Geophys. Res. 107 (2002), doi:10.1029/2001JB000486.
[25] V.A. Shashkanov, V.V. Metallova, Violation of Thellier's law for partial thermoremanent magnetizations, Izv. Acad. Sci. USSR Phys. Solid Earth Engl. Trans. 3 (1972) 80–86.
[26] A.S. Bol'shakov, V.V. Shcherbakova, A thermomagnetic criterion for determining the domain structure of ferrimagnetics, Izv. Acad. Sci. USSR Phys. Solid Earth Engl. Trans. 15 (1979) 111–117.
[27] V.P. Shcherbakov, E. McClelland, V.V. Shcherbakova, A model of multidomain thermoremanent magnetization incorporating temperature-variable domain structure, J. Geophys. Res. 98 (1993) 6201–6216.
[28] P. Riisager, J. Riisager, Detecting multidomain magnetic grains in Thellier paleointensity experiments, Phys. Earth Planet. Inter. 125 (2001) 111–117.
[29] V.V. Shcherbakova, V.P. Shcherbakov, F. Heider, Properties of partial thermoremanent magnetization in pseudosingle domain and multidomain magnetite grains, J. Geophys. Res. 105 (2000) 767–781.
[30] R.F. Butler, S.K. Banerjee, Theoretical single-domain size range in magnetite and titanomagnetite, J. Geophys. Res. 80 (1975) 4049–4058.
[31] W. O'Reilly, Magnetic minerals in the crust of the Earth, Rep. Prog. Phys. 39 (1976) 857–908.
[32] D.J. Dunlop, O. Özdemir, Rock Magnetism: Fundamentals and Frontiers, Cambridge University Press, 1997, 563 pp.
[33] C.M. Schlinger, D.R. Veblen, J.G. Rosenbaum, Magnetism and magnetic mineralogy of ash flow tuffs from Yucca Mountain, Nevada, J. Geophys. Res. 96 (1991) 6035–6052.

[34] C.M. Schlinger, J.G. Rosenbaum, D.R. Veblen, Fe-oxide microcrystals in welded tuff from southern Nevada; origin of remanence carriers by precipitation in volcanic glass, Geology 16 (1988) 556–559.
[35] R.B. Ellwood, Estimates of flow direction for calc-alkaline welded tuffs and paleomagnetic data reliability from anisotropy of magnetic susceptibility measurements: Central San Juan Mountains, southwest Colorado, Earth Planet. Sci. Lett. 59 (1982) 303–314.
[36] R. Leonhardt, C. Heunemann, D. Krása, Analyzing absolute paleointensity determinations: acceptance criteria and the software ThellierTool4.0, Geochem. Geophys. Geosyst. 5 (2004) Q12016, doi:10.1029/2004GC000807.
[37] D. Krása, C. Heunemann, R. Leonhardt, N. Petersen, Experimental procedure to detect multidomain remanence during Thellier–Thellier experiments, Phys. Chem. Earth 28 (2003) 681–687.
[38] J.G. Königsberger, Die Abhängigkeit der natürlichen remanenten Magnetisierungen bei Eruptivgesteinen von deren Alter und Zusammensetzung, Beitr. Angew. Geophys. 5 (1936) 193–246.
[39] P.A. Selkin, J.S. Gee, L. Tauxe, W.P. Meurer, A.J. Newell, The effect of remanence anisotropy on paleointensity estimates: a case study from the Archean Stillwater Complex, Earth Planet. Sci. Lett. 183 (2000) 403–416.
[40] E. McClelland-Brown, Experiments on TRM intensity dependence on cooling rate, Geophys. Res. Lett. 11 (1984) 205–208.
[41] M.H. Dodson, E. McClelland-Brown, Magnetic blocking temperatures of single-domain grains during slow cooling, J. Geophys. Res. 85 (1980) 2625–2637.
[42] V. Bouska, Natural Glasses, Ellis Horwood, New York, 1993, 354 pp.
[43] M. Wilding, D.B. Dingwell, R. Batiza, L. Wilson, Cooling rates of hyaloclastites: applications of relaxation geospeedometry to undersea volcanic deposits, Bull. Volcanol. 61 (2000) 527–536.
[44] J. Gottsmann, D.B. Dingwell, Cooling dynamics of spatter-fed phonolite obsidian flows on Tenerfie, Canary Islands, J. Volcanol. Geotherm. Res. 105 (2001) 323–342.
[45] J. Gottsmann, D.B. Dingwell, The thermal history of a spatter-fed lava flow: the 8-ka pantellerite flow of Mayor Island, New Zealand, Bull. Volcanol. 64 (2002) 410–422.
[46] J. Gottsmann, A.J.L. Harris, D.B. Dingwell, Thermal history of Hawaiian pa-hoehoe lava crusts at the glass transition: implications for flow rheology and emplacement, Earth Planet. Sci. Lett. 228 (2004) 343–353.
[47] C.M. Schlinger, D. Griscom, G.C. Papaefthymiou, D.R. Veblen, The nature of magnetic single-domains in volcanic glasses of the KBS Tuff, J. Geophys. Res. 93 (1988) 9137–9156.
[48] J. Gee, D.V. Kent, Magnetic hysteresis in young mid-ocean ridge basalts: dominant cubic anisotropy? Geophys. Res. Lett. 22 (1995) 551–554.
[49] J. Carlut, D.V. Kent, Paleointensity record in zero-age submarine basalt glasses: testing a new dating techinque for recent MORBs, Earth Planet. Sci. Lett. 183 (2002) 389–401.
[50] L. Tauxe, J.J. Love, Paleointensity in Hawaiian Scientific Drilling Project Hole (HSDP2): results from submarine basaltic glass, Geochem. Geophys. Geosyst. 4 (2003) 8702, doi:10.1029/2001GC000276.
[51] R.S. Coe, S. Grommé, E.A. Mankinen, Geomagnetic paleointensities from radiocarbon-dated lava flows on Hawaii and the question of the Pacific nondipol low, J. Geophys. Res. 83 (1978) 1740–1756.